Chapter 5 Failure Analysis of FRP Composite Tee-joint

5.1 Introduction

The last two three decades has seen extensive application of adhesive bonded technology in weight saving structures reducing both time, material and above all manufacturing costs. Adhesion methodology has become so versatile and such diversified into the new frontiers of aerospace, marine and automotive applications for joining of composite-composite and composite-metal structural parts thereby rendering inconclusive failure and fracture behavior coming into play limiting their proposed life span. Though it is not unknown that joint configuration, interface bonding chemistry and joining process, thermo-elastic material properties of adherend and substrate, edge conditions and geometry of joint, adherend and bond line and ply stacking of constituent laminae affects the performance and reliability of adhesively bonded joints, however the uncertainty of their failure and mixed-mode fracture phenomena has limited their full potential in many other applications. It is apprehended that either the earlier nomenclatured bonding parameters need to be reanalyzed in view of new design requirements or else there might be some new adhesion mechanism controlling the stress and deformation characteristics of these bonded structures. For eg. such integral phenomenon as bimodularity of interface due to variation of elastic modulus in tension and compression and curing stresses arising out of the mismatch of thermo-elastic material properties of adhesive and adherend ply stacking and lamina orientation. Therefore, the impetus of the present study has been to address these issues pertinently viz a viz a bimodular functionally graded adhesive tee joint. These joints are out-of-plane joints comprising of a right angled center plate adhesively bonded to a base plate. When compared to mechanically fastened joints, apart from the advantage of reduced body mass and cost, the adhesive bonded joints have the ability to transfer uniform load over the bonded area with fewer source of stress concentrations near joints, higher toughness and better corrosion and fatigue strength. However, the stress distribution in the bond line adhesive is non-uniform and is significantly affected by material modulus and thermal expansion properties. Even in an unloaded state, the tee configuration is not free to expand when loaded thermally, thereby inducing thermal stresses. The difference in thermal expansion coefficients of joint constituents might also invoke curing stresses, when the structure is cured for several hours from a higher temperature to lower temperature during manufacturing stages. Functionally graded adhesives have been evolved as a solution for obtaining uniform stress density along the bond line thereby substituting conventional single phase adhesives. Clearly, different parts of these tee joints are subjected to tension and compression asymmetrically, even when the mechanical loading is uniaxial mostly. The stress, deformation and subsequent failure and fracture characteristics then has a strong bearing on the pattern of material modulus exhibited by corresponding stress strain slopes. Hence, this modified stress dependent elasticity problem has to be addressed properly for enhancing joint reliability and design. Not only anisotropic and orthotropic materials such as composites, but also some traditional isotropic materials as ceramics, graphites and so on may also have different moduli in tension and compression. Realistically saying, most materials at elemental scale has some bimodulus characteristics refining the statement that compression and tension loading and unloading behavior are inherently two different phenomena.

5.2 Numerical analysis

First set of finite element analysis is performed for a purely mechanical loading in the form of load applied of 50N in y-direction at the top edge of substrate. The loading and boundary conditions are specified in Figure 5.1. Dimensions of different parts of tee-joint model are shown in Table 5.1. The test is terminated when the debonding is observed between adhesive and plate. Delaminations at the interfaces of main plate and adhesive, and adhesive and substrate have been analyzed both for mechanical loading in the first step and sequential thermo-mechanical loading in the second step. For studying the thermo-elastic stress behavior, in the second set, the mechanical loading is applied subsequent to the uniform temperature drop from the stress-free state at 300^0 C to the 30^0C room temperature to induce thermal residual stresses in the joint.

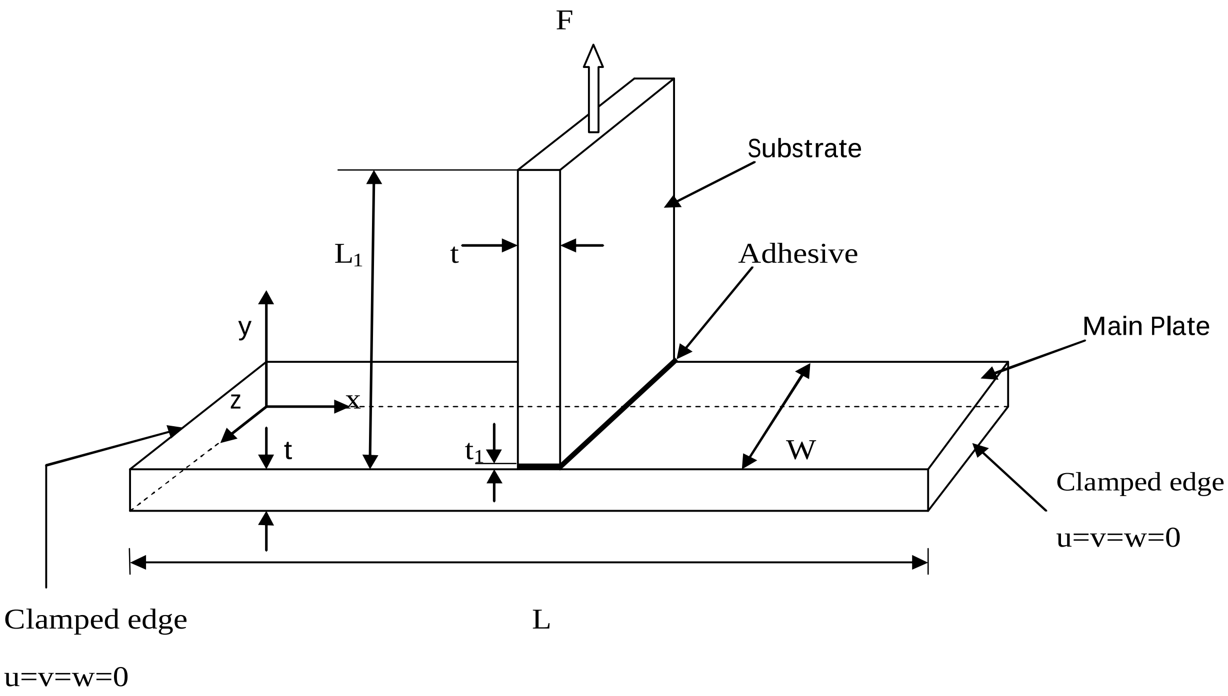

Figure 5.1 Configuration of tee-joint

Table 5.1 Dimensions of tee joint model

Parameters	Dimensions (mm)
Plate thickness, t	2.1
Adhesive thickness, t_1	0.2
Main plate length, L	100
Substrate length, L_1	30
Joint width	25

Table 5.2 Thermo-elastic material properties [127]

	Graphite/Epoxy	**Epoxy Adhesive**
Elastic Properties		
E_x (GPa)	127.50	E = 2.8 (GPa)
E_y (GPa)	9.00	
E_z (GPa)	4.80	
$G_{xy} = G_{xz}$ (GPa)	4.80	G = 1.42 (GPa)
G_{yz} (GPa)	2.55	
$\nu_{xy} = \nu_{xz}$	0.28	$\nu = 0.40$
ν_{yz}	0.41	
Thermal Properties		
α_x (/^{o}C)	4.3 X 10^{-6}	α = 62 X 10^{-6} (/^{o}C)
α_y (/^{o}C)	1.2 X 10^{-}6	
α_z (/^{o}C)	0.9 X 10^{-6}	
Temperature state:		

Curing temperature = 300°C

Room temperature = 30°

ΔT = -270°C

Bond layer is graded with functionally graded bimodular adhesive. It is implemented through continuous variation of elastic modulus along bond line which is governed by linear function profile (Equation 3.15). The Poisson's ratio for tension is considered as 0.4 and Poisson's ratio for compression ν_C can be calculated with the help of relation defined in Equation (3.19). The adhesive layer used for bonding is made of FGA whose properties vary from material 1 to material 2. Material gradients measured in terms of bimodulus ratio 'R' which varies from 1 to 5. The upper bound modulus $E_2(I)$ is taken as 2.8 GPa and lower bound modulus $E_1(I)$ is varied according to bimodulus ratio 'R' as expressed in Equation (3.17). Tension and compression parts of the adhesive layer have been modeled separately according to the equation given below [51]:

$$h_T = \frac{\sqrt{E_C}}{\sqrt{E_C}+\sqrt{E_T}}h \text{ and}$$

$$h_C = \frac{\sqrt{E_T}}{\sqrt{E_C}+\sqrt{E_T}}h \tag{5.1}$$

where E_T - modulus of elasticity for tension

E_C - modulus of elasticity for compression

h_C - height of the beam above neutral axis in compression region

h_T - height of the beam below neutral axis in tension region

h – total height of the beam ($h_T + h_C = h$)

A three-dimensional mesh is created of tee-joint is shown in Figure 5.2. Figure shows the zoomed view of finite element (FE) model developed for studying the thermo-elastic effect on fracture crack growth behavior of graphite/epoxy laminate specimen. It shows the details of deformed model of damaged specimen in the vicinity of crack tip. The final model has 36645 elements and 198874 nodes, yielding a total of 596622 degrees of freedom.

The important aspect of FEA is discretization and error analysis. This has been done extensively to achieve the optimized values of stresses. Relevant error analyses and mesh refinements have been carried out for a convergence of 0.001% on strain energy release rates along the delamination front. This has been achieved by taking an element size near the delamination front to be nearly equal to be one-quarter of the individual ply thickness along the plane of delamination [175-179]. To capture the delamination region stress field and avoid the oscillatory nature of the stresses very near to the crack front, this element size is found to be sufficient. Progressive mesh refinements have been made judiciously from delamination front to the laminate boundary. This scientifically graded mesh pattern significantly reduces the burden of computational effort necessary for an otherwise thermo-elastic fracture analysis (Figure 5.2).

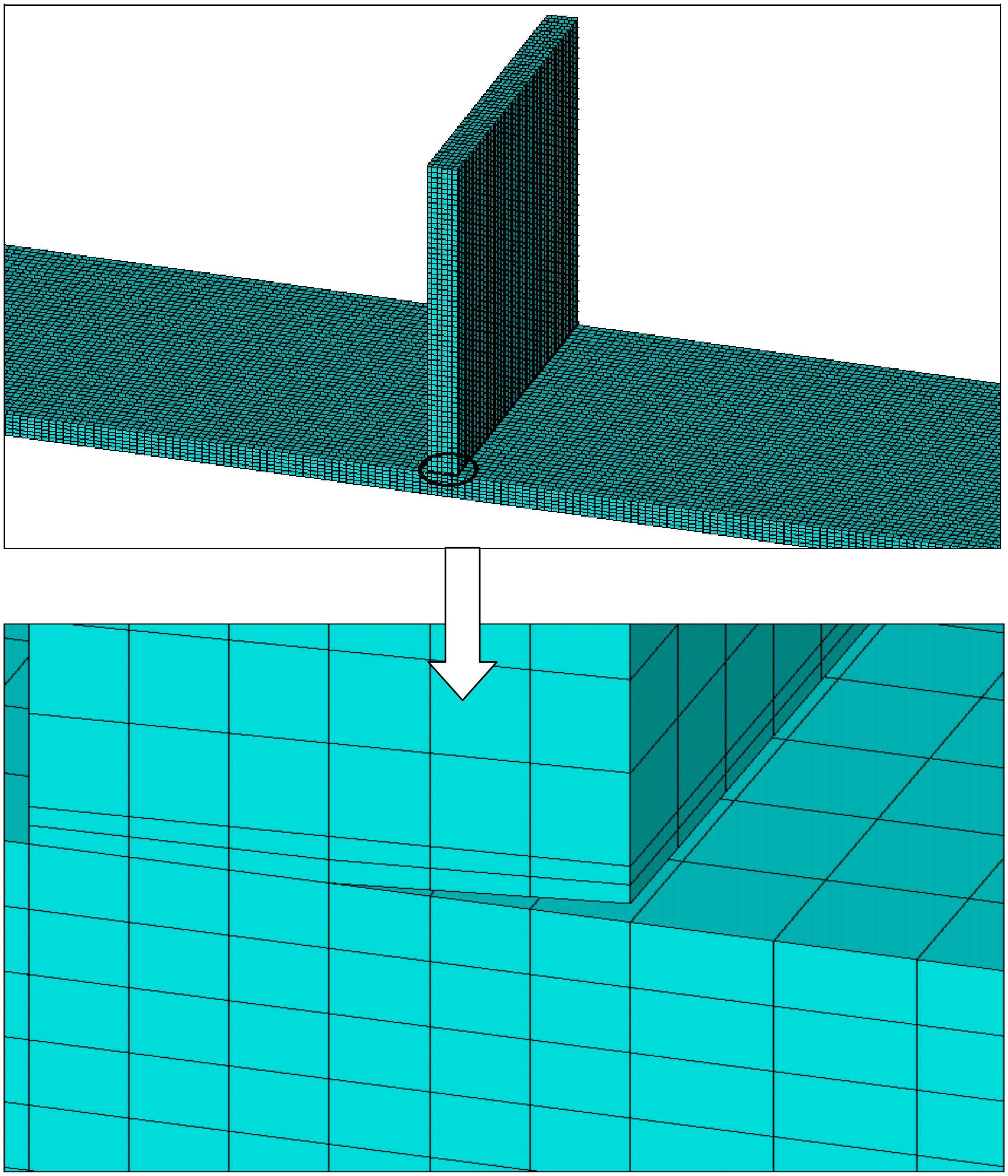

Figure 5.2 Zoomed view of FE model of the damaged specimen of tee-joint at the vicinity of crack tip

5.3 Results and discussion

In nonlinear finite element analyses, strain energy release rates are usually computed for unimodular adhesive. While in the present analysis, the results have been evaluated for the functionally graded bimodular behavior of the adhesive. The objective of this study is to signify the 3D modeling technique for the investigation of delamination from the initial crack in tee-joint. Full 3D thermo-elastic finite element analyses have been conducted to account the Strain Energy Release Rate (SERR) due to the curing stresses on tee-joint specimen with bimodular adhesive. Curing stresses are also known as the induced residual thermal stresses. Mode I, Mode II and Mode III strain energy release rates predominantly spread over a subsequential zone of delamination front. The asymmetric distributions are found to be different for different types of loading and bimodular ratios. Also, the total energy release rate $G_T = G_I + G_{II} + G_{III}$, along the bondline of the specimen is obtained from 3D analysis. The delamination is considered at the interfaces of main plate and epoxy ($y = 2.1$ mm) and epoxy and substrate ($y = 2.3$ mm). The value of G is determined at both interfaces and compared. The distribution of individual modes of strain energy release rate along the delamination front for different loading conditions on laminated composite have been discuss below.

5.3.1 Tee-joint delamination with mechanical load

The failure analyses indicate that the critical locations for the onset of interfacial failure front. Individual modes of SERR, G_I, G_{II} and G_{III} considered as fracture parameters governing the propagation of damages, have been computed along the interfacial failure front. Figure 5.3 exhibits the variations of G_I, G_{II}, G_{III} and G_T at the interface of main plate and bimodular epoxy with the varied bimodular ratio R under mechanical loading.

G_I takes the leading role for the propagation of interfacial failure. Referring to figure, it can be concluded that SERR values are kept on decreasing as the values of bimodular ratio R increases. This behavior is in good agreement with the result observed by Nimje and Panigrahi [127] for crack growth analysis of tee-joint. G_T is highest for the unimodular epoxy and keeps on decreasing for other values of R and moreover its value is approximately same for R=2 to 5. From Figure 5.3(b), it is clear that the peak value of ERR is at the edge ($z = 0.0$ mm and $z = 25.0$ mm). While in case of G_{III} , its lowest value is near free edges and middle portion of the tee-joint (Figure 5.3(c)). In Fig. 5.3 (b) and (c), there is a variation of Mode II & III SERR along interfacial failure front, respectively. It can be noted from figure that value of G_{II} is highest at the free edge i.e. z= 0 and 25.4 mm for all values of R. G_{III} value is lower at the free edge and mid part of failure front.

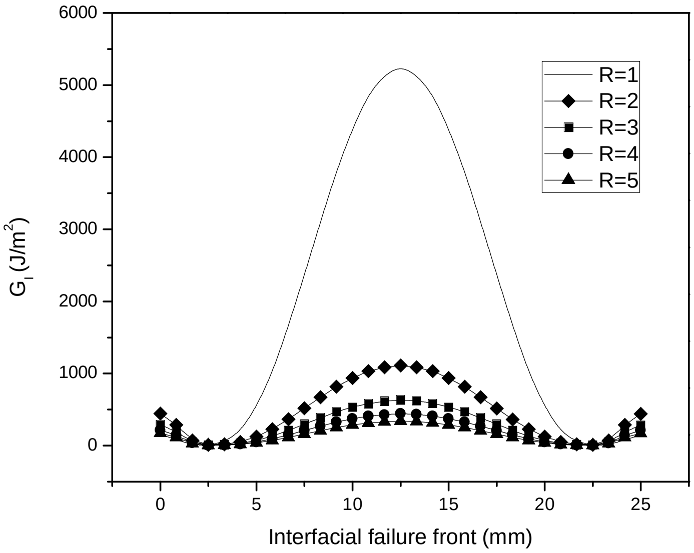

(a)

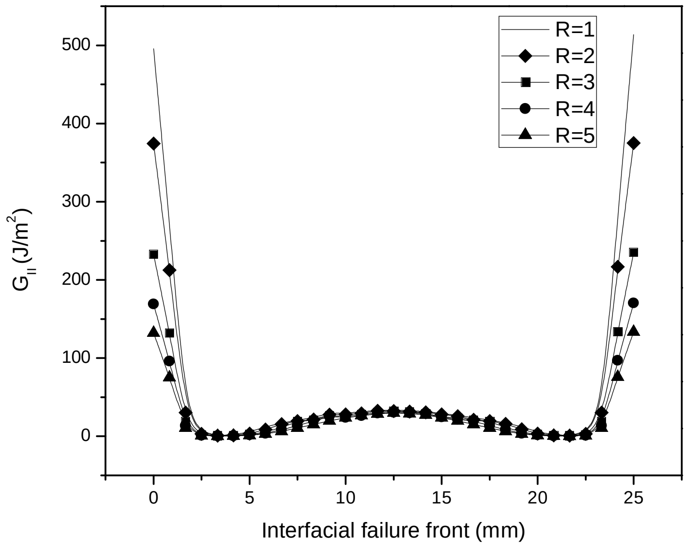
R=1
R=2
R=3
R=4
R=5
G_{II} (J/m^2)
500
400
300
200
100
0
0
5
10
15
20
25
Interfacial failure front (mm)

(b)

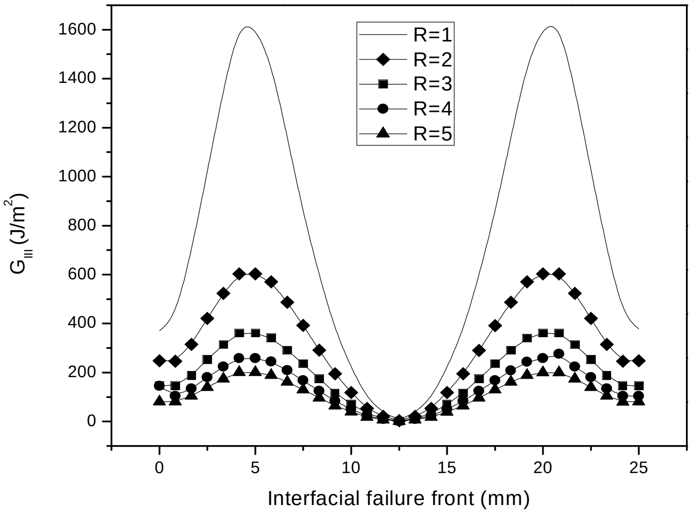
R=1
R=2
R=3
R=4
R=5
G_{III} (J/m^2)
1600
1400
1200
1000
800
600
400
200
0
0
5
10
15
20
25
Interfacial failure front (mm)

(c)

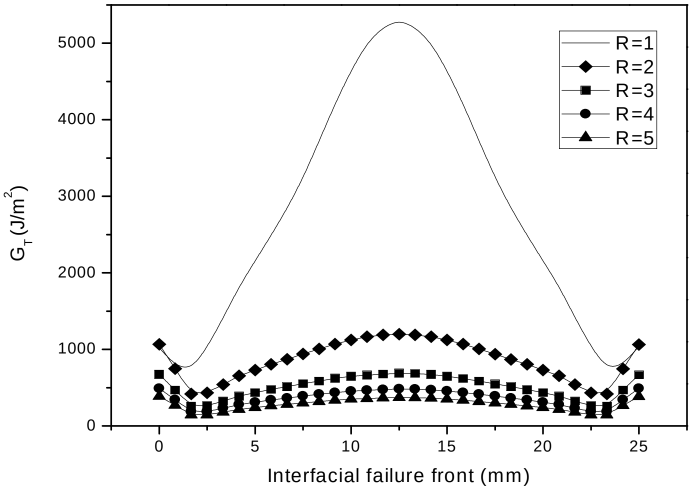

(d)

Figure 5.3 SERR along the interface of main plate and adhesive for varied bimodular ratio 'R' in functionally graded bimodular adhesively bonded tee-joint under mechanical loading (a) Mode I SERR (b) Mode II SERR (c) Mode III SERR (d) Total SERR

It is clear from Figure 5.4 that the dominance of failure is at the interface of main plate and adhesive layer in comparison to the epoxy-substrate interface for all value of R under mechanical loading. All the results follow the same trend, moreover the value of maximum energy release rate keeps on decreasing with R =1 to 5. There is a significant difference in the values of G for the two interfaces for all values of R. On comparing the total SERR for different R at $y = 2.3$ mm, graph follows the same pattern as in case of $y = 2.1$ mm but in this case, value of G is low (Figure 5.5). Here also the energy release rate is appreciably high for unimodular epoxy than the other values of bimodular ratio.

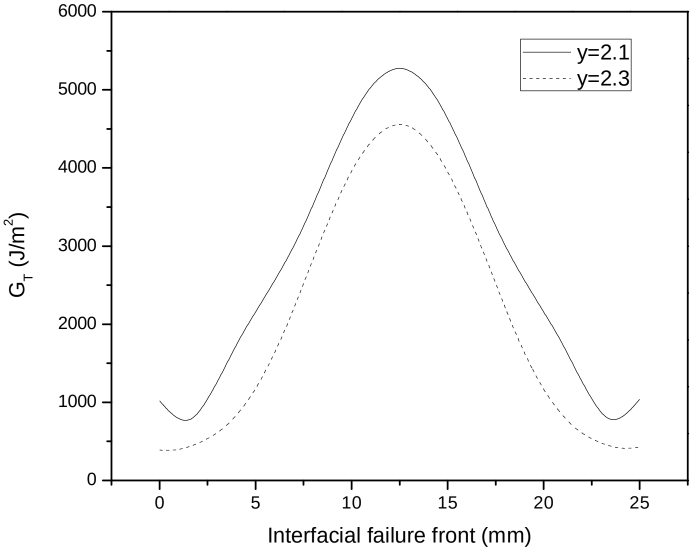
6000
5000
4000
3000
2000
1000
0
G_T (J/m^2)
0
5
10
15
20
25
Interfacial failure front (mm)
y=2.1
y=2.3

(a)

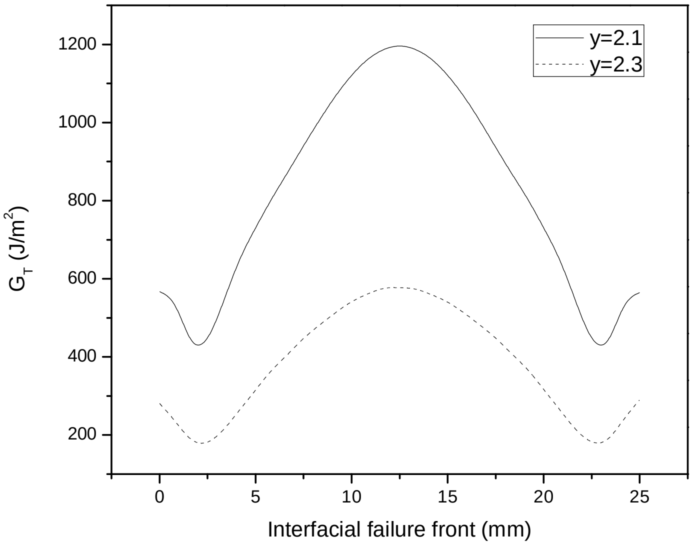
1200
1000
800
600
400
200
G_T (J/m^2)
0
5
10
15
20
25
Interfacial failure front (mm)
y=2.1
y=2.3

(b)

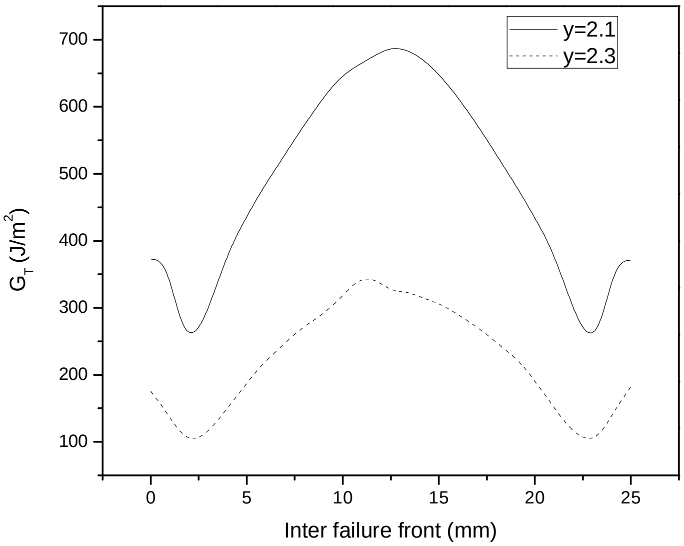
y=2.1
y=2.3
700
600
500
400
300
200
100
0
5
10
15
20
25
G_T (J/m^2)
Inter failure front (mm)

(c)

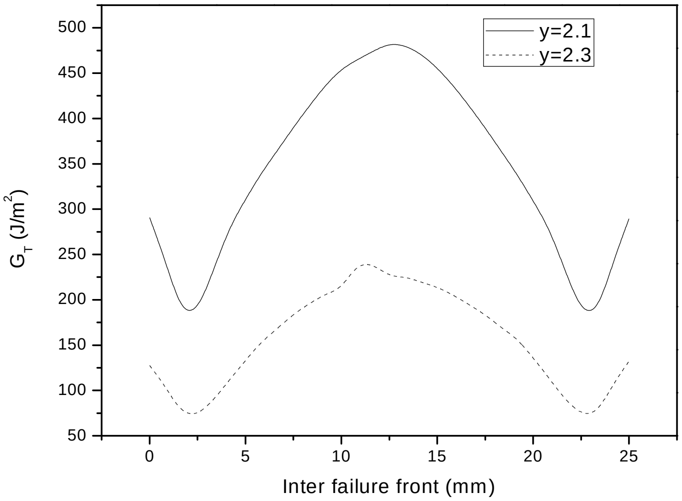
y=2.1
y=2.3
500
450
400
350
300
250
200
150
100
50
0
5
10
15
20
25
G_T (J/m^2)
Inter failure front (mm)

(d)

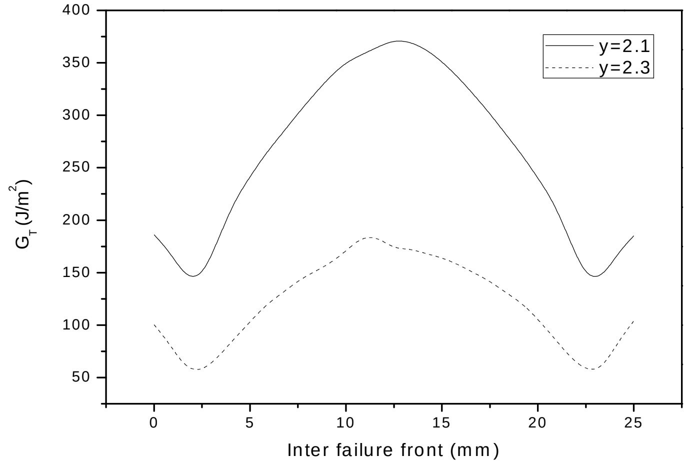

(e)

Figure 5.4 Effect of the position of delamination on total SERR at various bimodular ratio under mechanical loading (a) R =1, (b) R =2, (c) R =3, (d) R =4, (e) R =5

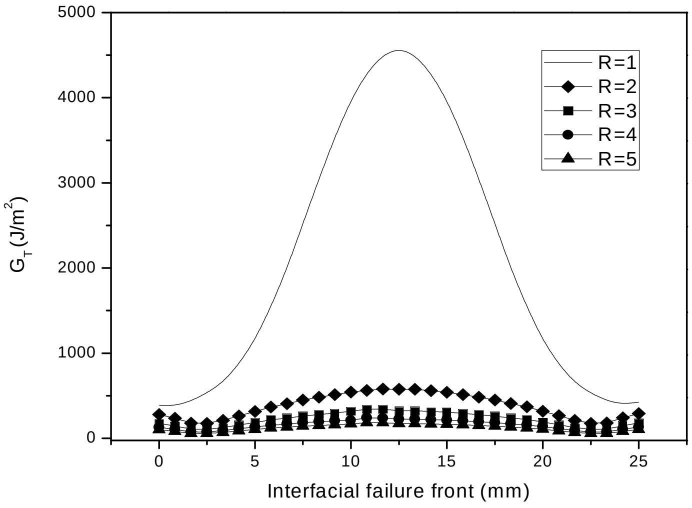

Figure 5.5 Comparison of Total SERR for various R at y =2.3mm under mechanical loading

5.3.2 Tee-joint delamination with coupling effect of curing stresses and axial loading

Different modes of strain energy release rate are examined by the virtual crack closure technique (VCCT) for modeled delamination. The SERR along the failure front are plotted for $y = 2.1$ mm under thermo-mechanical loading in Figure 5.6. After a small initial drop the evaluated total energy release rate increases sharply with delamination length, reaches a peak value and gradually decreases. All the figures plotted below follow the same configuration as in case of mechanical loading. Referring to the Figs. 5.7(a)-(e), it may be noted that loci of the total SERR (G_T) values are continuously reducing for a varied gradation and bimodularity of material properties of the adhesive irrespective of the position of delamination. This indicates that the driving forces are continuously decreasing with respect to bimodular ratio. There is a significant difference in the values of G for two interface delamination position but the nature of graph is almost same for different values of R. In case of Figure 5.8, G_T versus x curve reaches a peak along delamination length and then decreases. It is obvious that the value is much high for $R = 1$ in comparison of other values of R.

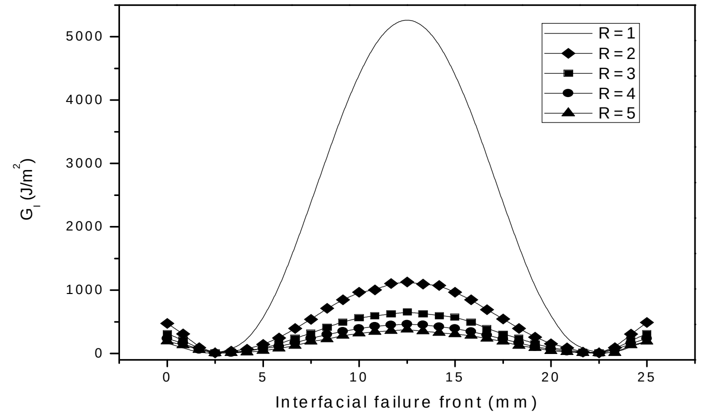

(a)

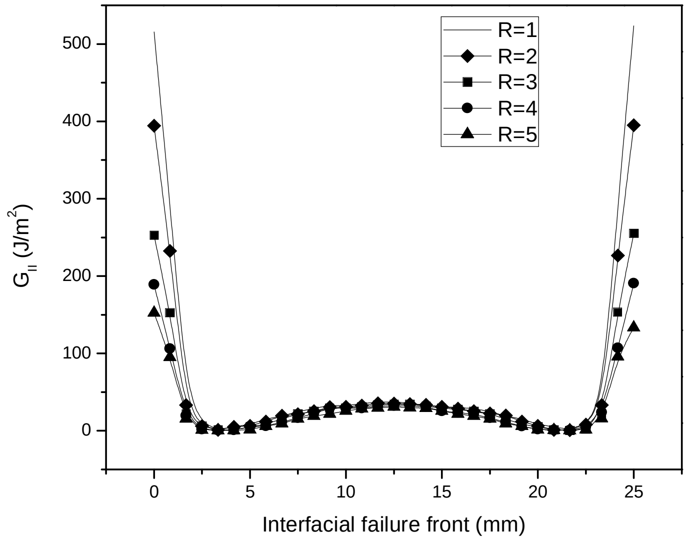
R=1
R=2
R=3
R=4
R=5
G_{II} (J/m^2)
500
400
300
200
100
0
0
5
10
15
20
25
Interfacial failure front (mm)

(b)

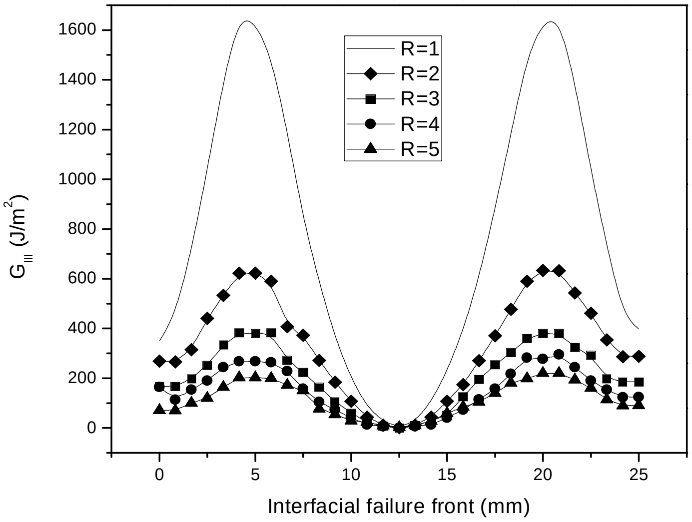
R=1
R=2
R=3
R=4
R=5
G_{III} (J/m^2)
1600
1400
1200
1000
800
600
400
200
0
0
5
10
15
20
25
Interfacial failure front (mm)

(c)

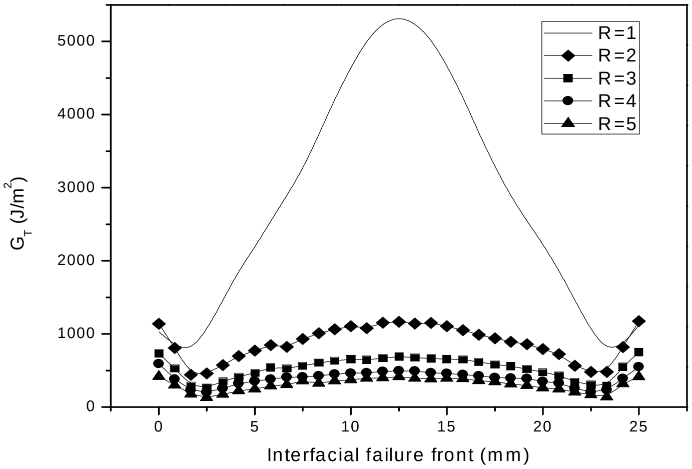

(d)

Figure 5.6 SERR along the interface of main plate and adhesive for varied bimodular ratio '*R*' in functionally graded bimodular adhesively bonded tee-joint under thermo-mechanical loading (a) Mode I SERR (b) Mode II SERR (c) Mode III SERR (d) Total SERR

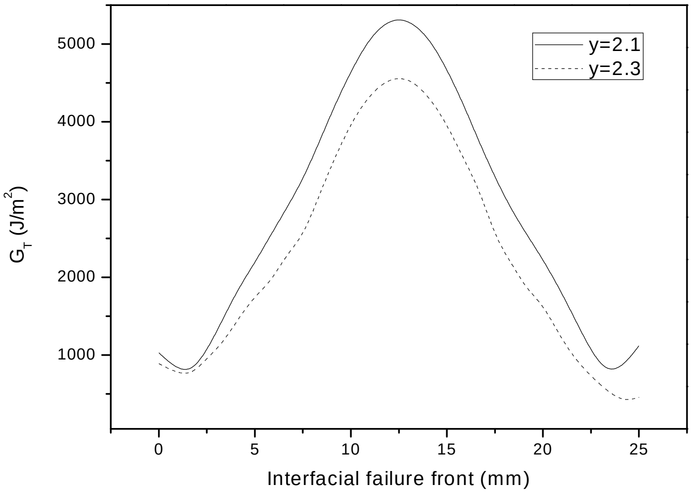

(a)

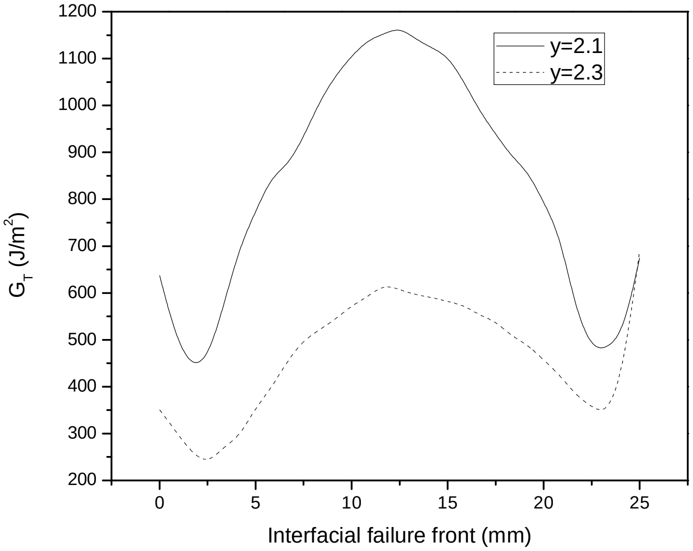
y=2.1
y=2.3
G_T (J/m^2)
1200
1100
1000
900
800
700
600
500
400
300
200
0
5
10
15
20
25
Interfacial failure front (mm)

(b)

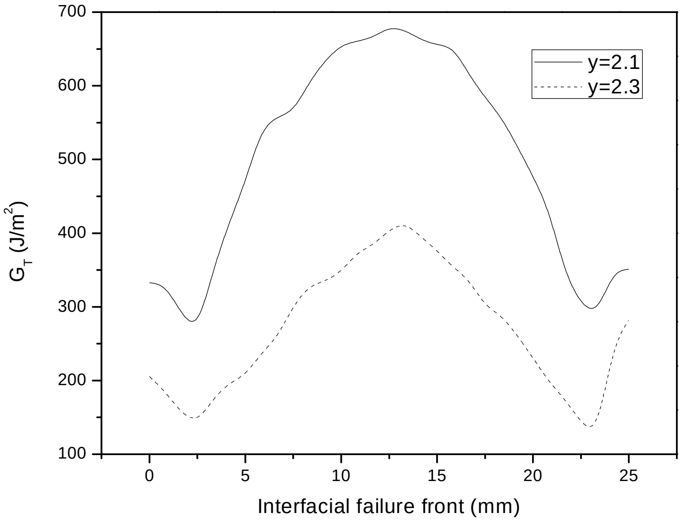
y=2.1
y=2.3
G_T (J/m^2)
700
600
500
400
300
200
100
0
5
10
15
20
25
Interfacial failure front (mm)

(c)

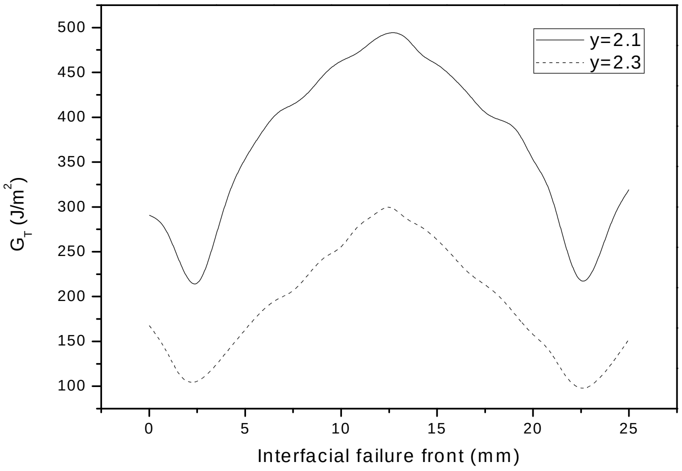

(d)

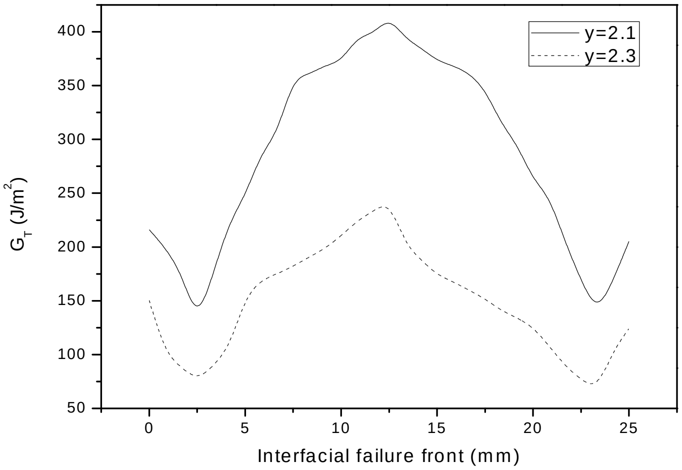

(e)

Figure 5.7 Effect of the position of delamination on total SERR at various bimodular ratio under thermo-mechanical loading (a) $R=1$, (b) $R=2$, (c) $R=3$, (d) $R=4$, (e) $R=5$

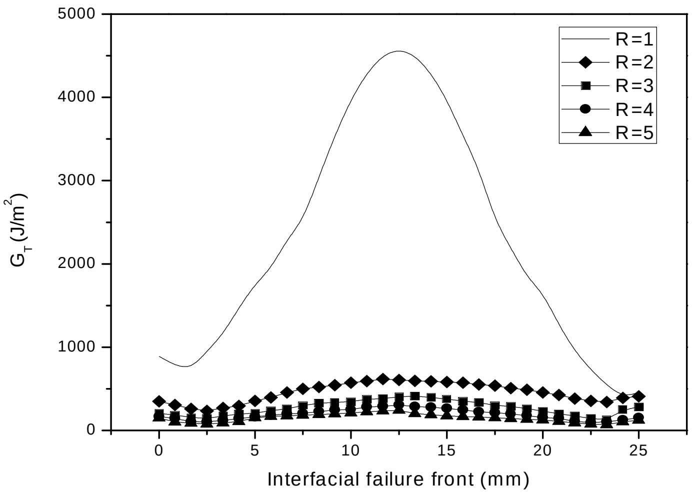

Figure 5.8 Comparison of Total SERR for various R at y =2.3mm under thermo-mechanical loading

5.3.3 Comparison of tee-joint delamination with and without considering the coupling effect of curing stresses and axial loading

In the present work, bimodularity of the adhesive is continuously and smoothly varied along the failure front using appropriate linear function profile (Equation 3.15). In Figure 5.9, the comparison is done for total SERR under mechanical and thermo-mechanical loading for different values of R. It may be concluded from figures that G value is little bit high for coupled field than mechanical under all values of R. All the results have same manner of variation that the maximum rate of delamination is at the center of the bondline i.e. at 12.5 mm (approximately). It is interesting to note that the coupling effect of curing stresses in some cases, enhances the mixed mode interlaminar delamination crack growth, whereas in others, it also opposes the interface crack growth mechanism depending the location of the delamination front in between epoxy and plate.

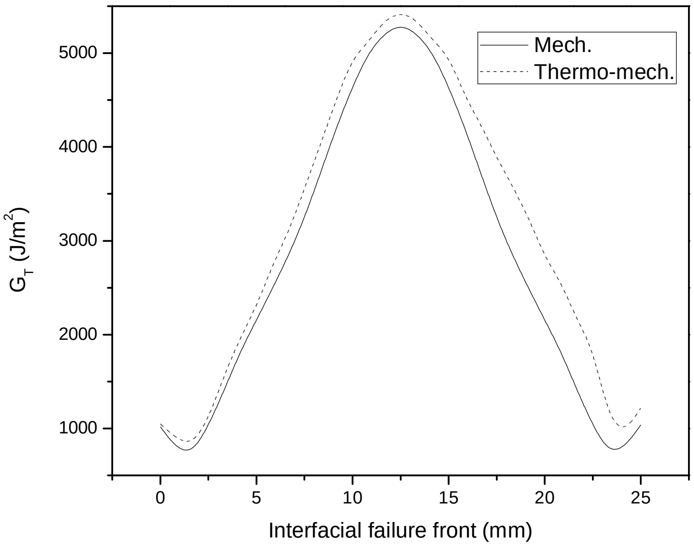
Mech.
Thermo-mech.
G_T (J/m^2)
5000
4000
3000
2000
1000
0
5
10
15
20
25
Interfacial failure front (mm)

(a)

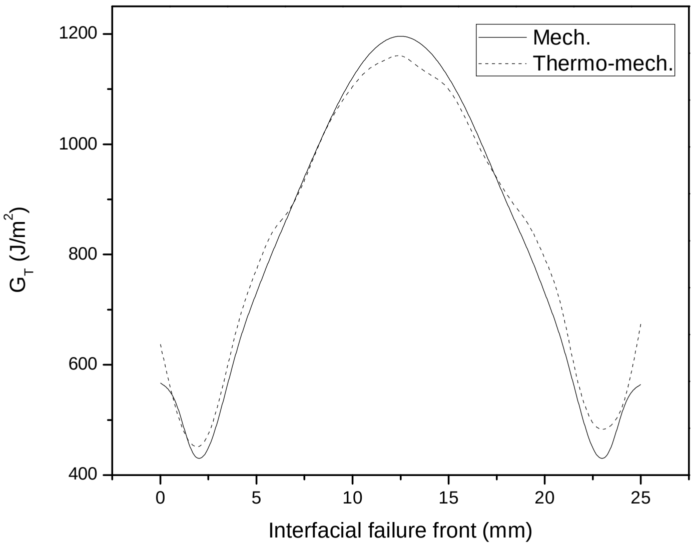
Mech.
Thermo-mech.
G_T (J/m^2)
1200
1000
800
600
400
0
5
10
15
20
25
Interfacial failure front (mm)

(b)

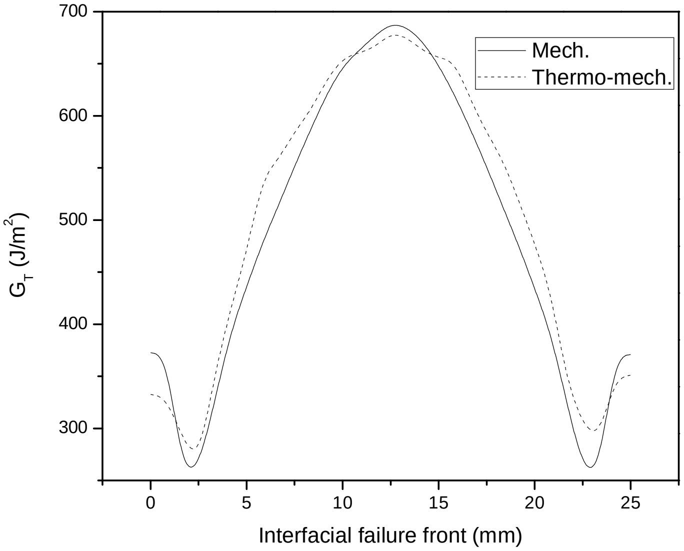
700
600
500
400
300
G_T (J/m^2)
0
5
10
15
20
25
Interfacial failure front (mm)
Mech.
Thermo-mech.

(c)

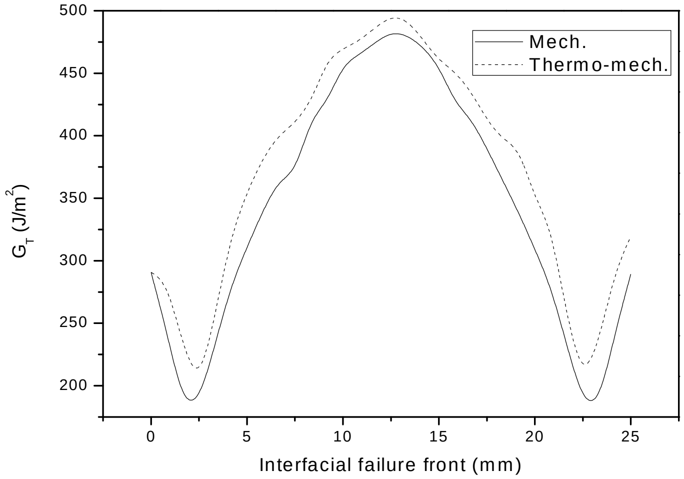
500
450
400
350
300
250
200
G_T (J/m^2)
0
5
10
15
20
25
Interfacial failure front (mm)
Mech.
Thermo-mech.

(d)

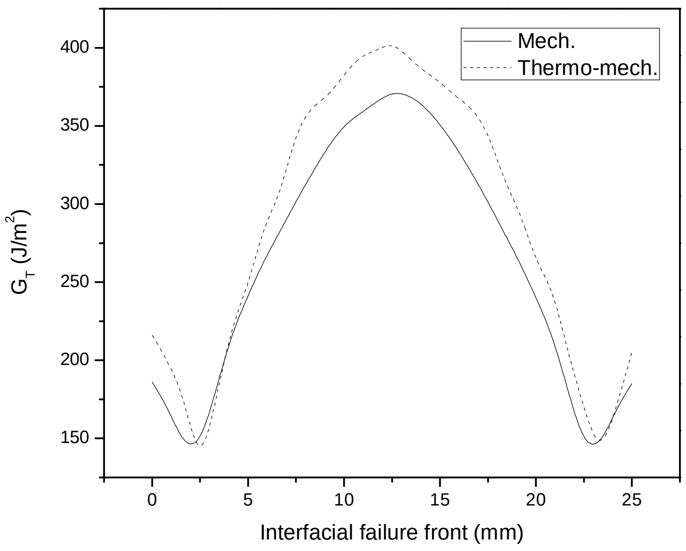

(e)

Figure 5.9 Effect of mechanical and thermo-mechanical loading on total SERR at y =2.1mm with various bimodular ratio (a) R =1, (b) R =2, (c) R =3, (d) R =4, (e) R =5

5.4 Conclusion

This research work presents interfacial failure analysis of functionally graded FRP composite tee joint structure with bimodular adhesive to indentify the critical location for damage onset. The desirable intention of the tee joint designer is to retard interfacial failure propagation rate in order to intensify the structural integrity of the tee joint. As a result, the strength and lifetime of the tee joint structure can be significantly upgraded. In the present research, efforts are made to retard interfacial failure propagation rate by employing functionally graded bimodular adhesive along the delamination line. The influence of interaction of thermal and elastic field on the delamination progression characteristics of bimodular interface tee-joints have been demonstrated by delineation of SERR plots along the interface. The following specific conclusions are drawn on results and observations.

1. Significant difference in energy release rate along the interfacial delamination front has been observed between mechanical and thermo-mechanical fracture behavior while considering the effect of curing stresses and mechanical loading in tandem. The fracture parameter strain energy release rate G_T exhibits non-uniform variation when the bimodular ratio varies from $R = 1$ to $R = 5$, though the maximum is occurring between delamination front 10 to 15 mm for all ply configurations. These asymmetries in the interface fracture behavior are reasoned to be the effect of anisotropy ratio of thermal expansion coefficients and influence coefficients of the multi-directional laminates with bimodular interfaces.

2. From the G_T distribution along the Interfacial failure front plot, it is seen that the peak of the distribution pattern is occurring at the center of the delamination front with an asymptotic variation at both the ends. This has been in contrast to the belief of constant strain energy release rate along the interface for self-similar crack front propagation. This uneven energy distribution pattern might lead to interfacial failure propagation characteristics which are geometrically non-self-similar for each subsequent interface delamination progression.

3. Mode I is the most dominant component of the total energy release rate and plays an important role in characterizing the delamination crack growth behavior and failure of composite laminates.

4. A functionally graded bimodular adhesively bonded tee joint has revealed significant reduction in damage growth driving forces compared to a unimodular adhesive. It has been concluded that the bimodularity and gradation of adhesive considerably reduces the failure

propagation rate but as we vary the bimodularity index from R =1 to 5, the bimodular effect is found to be more pronounced upon fracture energy distribution in comparison to functionally graded property. Therefore, the difference in tension and compression behavior of adhesive joints has to be appropriately calibrated for a more reliable fracture resistance design.

5. Damage is more pronounced along the interface of the main plate and adhesive compared to the adhesive and substrate interface.

6. Strain Energy Release Rate is more when coupling effect of curing stress is present than the elastic loading.

This work signifies the relative influence of induced curing stresses on the delamination propagation behavior in functionally graded bimodular adhesively bonded tee joint and therefore it should be taken into account in damage development studies of adhesive bonded joints. Fracture behavior and damage propagation in case of skin-stiffener should also be evaluated as adhesively bonded joints and it is included in advanced chapters.